第二届宝钢学术年会
The Second Baosteel Biennial Academic Conference

Proceedings

of the Second Baosteel Biennial Academic Conference

谢企华　徐乐江　主编
Edited by
XIE Qihua & XU Lejiang

Volume 2

会议主题：技术创新与循环经济
Theme: Technology Innovation and Circular Economy

上海科学技术文献出版社
Shanghai Scientific and Technological Literature Publishing House

第二届宝钢学术年会
The Second Baosteel Biennial Academic Conference

Proceedings

of the Second Baosteel Biennial Academic Conference

谢企华　徐乐江　主编
Edited by
XIE Qihua & XU Lejiang

Volume 2

会议主题：技术创新与循环经济
Theme: Technology Innovation and Circular Economy

时间：2006.5.25－26
地点：中国 上海 宝钢研究院
May 25 - 26, 2006
Baosteel Research Institute, Shanghai, China

上海科学技术文献出版社
Shanghai Scientific and Technological Literature Publishing House

2006.05.31. 贺.

编 委 会

主　　编:谢企华　徐乐江

常务主编:崔　健

编　　委:(按姓氏笔画为序)

马凯利　王　宁　王　喆　王仁意　王承学
王治政　方　园　孙全社　江来珠　刘宏娟
刘晓琼　任　燕　杜　斌　张　恺　张　毅
张永杰　邹　宽　余永桂　吴东鹰　陆匠心
陆祖英　宋洪伟　陈　静　陈英颖　陈建生
李仁江　庞远林　范朝晖　施胜洪　徐乐江
徐汝青　翁国强　黄宗泽　黄　剑　崔　健
谢企华　焦四海　蔡　宁　薛祖华

责任编辑:池文俊　翁国强　刘宏娟

Editorial Committee

Editors-in-Chief: XIE Qihua　XU Lejiang

Administrative Editor-in-Chief: CUI Jian

Members of Editorial Committee (in the order of stroke number of Chinese surname):

MA Kaili	WANG Ning	WANG Zhe	WANG Renyi
WANG Chengxue	WANG Zhizheng	FANG Yuan	SUN Quanshe
JIANG Laizhu	LIU Hongjuan	LIU Xiaoqiong	REN Yan
DU Bin	ZHANG Kai	ZHANG Yi	ZHANG Yongjie
ZOU Kuan	SHE Yonggui	WU Dongying	LU Jiangxin
LU Zuying	SONG Hongwei	CHEN Jing	CHEN Yingying
CHEN Jiansheng	LI Renjiang	PANG Yuanlin	FAN Zhaohui
SHI Shenghong	XU Lejiang	XU Ruqing	WEN Guoqiang
HUANG Zongze	HUANG Jian	CUI Jian	XIE Qihua
JIAO Sihai	CAI Ning	XUE Zuhua	

Executive Editors: CHI Wenjun　WENG Guoqiang　LIU Hongjuan

前　言

两年前的五月，这里曾经举办了首届宝钢学术年会，就“可持续的钢铁，可持续的未来”这一主题，开展了广泛的交流，得到了各界朋友们的大力支持和热情参与，收到了很好的效果，至今我们还记忆犹新。

今天，我们再次相聚在黄浦江畔，倍感愉快。本届年会的主题是“技术创新与循环经济”。这是上届年会主题的延伸和深化。在我们国家，正在执行着以人为本，全面、协调、可持续的科学发展观。国民经济新一轮的发展规划，对冶金界的节能降耗和环境保护，提出了更加严格的要求。

两年来，世界粗钢产量连续突破10亿和11亿吨，2005年比2004年又增长5.9%，其中有一半以上出产在亚洲地区；增长的部分几乎全部来自发展中国家。钢铁产品仍然具有十分广阔的市场空间；钢铁仍然是不可替代的工程材料；钢铁仍然对世界经济发展起着举足轻重的作用。

但是，人们也充分意识到，过大的资源消耗与过重的环境负担，已构成钢铁工业可持续发展的制约因素。要缓解这种制约、越过这一瓶颈，就要走节能降耗之路，就要走循环经济之路。要开辟这样的路，就只能靠技术进步与创新，靠技术创新来推动可持续发展。

本届年会共收到国内外作者的技术论文400余篇。经专家认真筛选，将其中的240篇收入本论文集中。论文集共分为3册。

在此，我们衷心感谢论文的作者、年会学术委员会成员、顾问、专家、筹备人员和论文集编辑人员为年会成功召开与论文集出版所做的贡献，因时间仓促，文集中缺点和错误在所难免，期盼大家提出宝贵的意见。

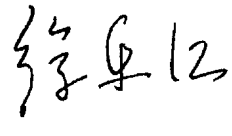

宝钢集团有限公司总经理

PREFACE

Two years ago in May, the first Baosteel Biennial Academic Conference (BAC) was held here, during which extensive exchanges were conducted on the theme of "the sustainable steel the sustainable future". The conference has achieved fruitful results thanks to the energetic support and active participation of friends from all walks of life, which still remains fresh in our memory.

Today, we are delighted to gather again on the riverside of Huangpu River. The theme of this conference is "technology innovation and circular economy", an extension and deepening of the theme of the previous BAC. A comprehensive, harmonious and sustainable scientific outlook on development featuring people first is being implemented in the country. The new round of development planning of national economy puts forward more stringent requirements on metallurgical industry for energy saving, consumption reduction and environmental protection.

The world crude steel output exceeded 1 and 1.1 billion tons respectively in the past two years. The year 2005 witnessed a global output increase by 5.9% over the previous year, almost all coming from developing countries and over half of which was contributed by Asia. There is still a big potential market for steel products; steel remains an irreplaceable engineering material; it still plays a vital role in the economic development of the world.

However, we fully recognize the fact that excessive energy consumption and overburden to the environment have constrained the sustainable development of steel industry. To relax the constraint and overcome the bottlenecks, we need to embark on a road of circular economy featuring energy saving and consumption reduction through technological progress and innovation which propel the sustainable development.

Among the over 400 technical papers contributed by both domestic and overseas authors, 240 of them have been chosen and placed in the proceedings (in three volumes) after a professional and careful selection.

Hereby, heartfelt gratitude is extended to authors, members of the academic committee of the conference, advisors, experts, staff of the preparatory committee and editing team of the proceedings, for their great devotion and contribution to the successful convening of the conference as well as the publication of the proceedings. Due to limitation of the time, the proceedings still have a great potential for further improvement. We are sincerely looking forward to your precious advices.

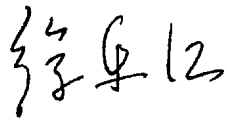

XU Lejiang

President of Baosteel Group Corporation

此为试读,需要完整PDF请访问: www.ertongbook.com

CONTENTS

Advanced Technology on Iron and Steel

1. Ultrafine Grained Steels Managing Both High Strength and Ductility ····· Nobuhiro TSUJI(1)
2. Grain Size Distribution Features and Yield Strength of Ultrafine-Grained Low Carbon Steels ····· Fuxing YIN *et al*(7)
3. Effect of Microstructure Refinement on Hydrogen Embrittlement of High Strength Martensitic Steel ····· Kaneaki TSUZAKI *et al*(12)
4. High Strength and Good Ductility of Bulk Nanostructured Metastable Austenitic Alloys ····· Jae-Eun JIN *et al*(18)
5. Development of Stable MIG Welding in Pure Ar Gas Using New-Hybrid Wire ····· Terumi NAKAMURA *et al*(22)
6. Large Strain-High Z Deformation Processing and Its Applications to Produce Large Scale Bulk Ultrafine Grained Steels ····· Shiro TORIZUKA *et al*(26)
7. Fracture of Ultrafine-grained Ferrite/Cementite Steel ····· Kotobu NAGAI *et al*(32)
8. Corrosion Resistance of Si and Al-bearing Ultrafine Grained Weathering Steel ····· T. NISHIMURA(37)
9. Formation of Naturally Deposited Films during Solidification and their Effect on Heat Transfer ····· Paolo NOLLI *et al* (42)
10. The Effect of Copper on Heat Transfer Behavior during Droplet Solidification ····· YU Yan *et al*(52)
11. Utilization of Impurity Elements in Steel by Rapid Solidification Process ····· LIU Zhongzhu *et al*(58)
12. Study Progress of Spray Forming Technology in Baosteel ····· FAN Junfei *et al*(64)
13. High Frequency Oscillation Phenomena in the Hartmann Resonance Tube ····· LI Bo *et al*(70)
14. Avoidance of Microstructural Heterogeneities by Hot Rolling Design in Thin Slab Direct Rolled Niobium Microalloyed Steels ····· P. URANGA *et al*(75)
15. A New Continuous Casting Mold Repairing Method- Cold Gas Dynamic Spray ····· ZHANG Junbao *et al*(81)

Metallurgical Equipment and Automation

16. Practice of Enlargement and Modification for Dwright-Lloyd Sintering Strands at Baosteel ····· WANG Yuefei *et al*(85)
17. Innovative Solutions for Advanced Steelmaking and Casting Technologies ··· Jens KEMPKEN *et al*(89)
18. The Technology of Circumfluence Control for Molten Steel in RH System ····· WU Jie(96)
19. VAI's Continuous Casting Technology How Competence Results in Client Satisfaction ····· Andreas FLICK *et al*(102)
20. High-Tech Solutions for the Upgrading of HSM ····· J. MAIERL *et al*(109)
21. Latest Developments in Hot Rolling Technology ····· Stephan KRÄMER(116)
22. Modernizing Automation and Drives of the Baoshan Tandem Cold Mill No. 1 ····· Josef HOFBAUER *et al*(126)

23. Improvement of Hot Dip Galvanizing Process by "Hot" Coating Weight Measuring and Control System ..... Joachim OLSCHEWSKI(130)
24. Temperature Stability in Galvanizing Pots as a Function of Power Supply Technology ..... Bill ROVINS(136)
25. New Coating Processes for Steel Strip ..... F. AREZZO *et al*(141)
26. Industrial PVD for Continuous Strip Coating Challenges and Solutions ..... Ulf SEYFERT *et al*(147)
27. Spotless Arc Activated Reactive Large Area EB – PVD of Titanium Oxide and Titanium Nitride ..... Christoph STEUER *et al*(152)
28. New Coating Systems for Steel Strips by Physical Vapor Deposition ..... B. SCHEFFEL *et al*(157)
29. Making Chinese Plate and Strip Production Even More Versatile at NISCO ..... Marcus BUERZLE *et al*(164)
30. Introduction of Performance and Advanced Application of Endless Bar Rolling System® ..... Susumu OKAWA(170)
31. Prospect of Construction of Equipment Diagnosis Center at Baosteel ..... LIU Yao *et al*(177)
32. Technical Features of Production Line for Trenchless Drill Pipe in Baosteel ..... FAN Yingqi *et al*(184)
33. From Surface Inspection Data to Surface Quality Yield Management ... Michael TRUNKHARDT (189)
34. New Technique Applied and Attained Design Production in Baosteel No. 4 BF ..... ZHU Renliang *et al*(199)
35. A Novel Approach to Skinpass Rolling Hot-dipping Zinc Strip ..... GU Tingquan *et al*(205)
36. The Integration Desing of Cold Mill Passschedule Calculation (in Chinese) ..... WU Wenbin *et al*(211)
37. The Power Problem of Carrousel Tension Reel in Tandem Cold Mill (in Chinese) ..... CHEN Zhiyin(216)
38. The Application of Equipment Fault Checking and Measuring Technic on Steel Rolling Manufacture (in Chinese) ..... ZHAO Yanlai *et al*(220)
39. The Influence on Electrical Drive by the Fluctuation of Voltage ..... HUANG Zhigang *et al*(223)
40. Application of High and Low Voltage Compensation Technology in Steel Rolling (in Chinese) ..... WANG Bing *et al*(228)
41. The First Trenchless Technology Drill Pipe End-upset Product Line in China (in Chinese) ..... PEI Zhiqiang *et al*(232)
42. Advanced BOF Dynamic Control System Integrating Slag Oxygen Potential ... Ken KATOGI *et al*(237)
43. The Prediction of Roll Force and Temperature during Heavy Plate Rolling ..... Changho MOON *et al*(241)
44. The Research and Application of MES Key Technology in Steel Enterprise ..... CONG Liqun *et al*(246)
45. Improvement of the Crown and Shape Control Model for the Hot Rolling ... Kanji HAYASHI *et al*(251)
46. Development and Application of the Profile and Flatness Simulator ..... Yhu-Jen HWU(257)
47. Study on Fuzzy Evaluation Method for Steelmaking and Continuous Casting Scheduling ..... CHEN Wenming *et al*(262)
48. The Factors Analysis of Various Working Procedures for the Converter-continuous Casting- Hot Rolling Production Organization Scheduling ..... LU Liming(268)
49. Study of Biting Steel control for Coiler's Wrapper Rolls ..... HUANG Ninghai *et al*(274)
50. Research and Application of Mathematical Models Related to Speed in Cold Rolling Process ..... ZHAO Huiping *et al*(281)
51. Multiple Coils Recognition System for Unmanned Crane Using Stereo Vision ... Dowan KIM *et al*(286)
52. Optimization Based Production and Logistics Scheduling in Steel Industry ..... TANG Lixin *et al*(293)

53. The Integrated Process Control System Solution of Baosight for Iron & Steel Enterprise ..... ZHU Xueqi *et al*(297)
54. Research and Application of Optimal Production Plan System in Baosteel (in Chinese) ..... DU Bin *et al*(303)
55. System Integrating Technology for the EIC Automatic Control System of Baosteel No. 4 Blast Furnace (in Chinese) ..... ZHU Xueqi *et al*(310)
56. Reheating-Furnace Control Model and Application for Baosteel Hot Strip Rolling Plant (in Chinese) ... LU Lihua *et al*(315)
57. Realization of the MES Working Procedure Plan in No. 3 Steelmaking Plant and Heavy Plate Plant of Jigang (in Chinese) ..... YAN Zongming *et al*(319)
58. Development and Integration of Process Control System for Hot Strip Rolling Plant (in Chinese) ..... SHAN Xuyi *et al*(323)
59. Application of Smith Predictor for Gauge Control in 2050mm Hot Strip Mill (in Chinese) ..... CHEN Zhirong *et al*(329)
60. The Strategy and Practice in the Revamp of EIC for the 2030 Cold Rolling Tandem Mill of Baosteel (in Chinese) ..... WANG Ruiting(334)
61. Strip Temperature Control Method for the Heating Section of a Continuous Annealing Line (in Chinese) ..... ZHOU Jiangang *et al*(340)
62. Several Important Problems in Data Mining to the Industrial Process (in Chinese) ..... GUO Zhaohui(344)
63. Design and Application of DCS Electric System in Gas and Stream Power Generation in Jigang (in Chinese) ..... GU Fangchun *et al*(347)
64. Analysis of Automatic Gauge Control Developing Process (in Chinese) ..... LI Yugui *et al*(351)
65. Structured Figurative Simulation of Rolling Process (in Chinese) ..... ZHENG Shenbai *et al*(359)
66. Industrial Intelligent Technology and Its Application in Metal Industry (in Chinese) ..... SUN Yanguang(364)
67. Design and Exploitation of the Strenghth Stability Control Model of Wire Rod Products for Twisting (in Chinese) ..... ZHU Xing'an(369)
68. Discussion on the Quality Control of High Speed Wire Rod (in Chinese) ..... WU Zhenping *et al*(374)

Ultrafine Grained Steels Managing Both High Strength and Ductility

Nobuhiro TSUJI

(**Dept. Adaptive Machine Systems, Osaka University, Suita** 565 - 0871, **Japan**)

Abstract: Mechanical properties of the ultrafine grained (UFG) steels having mean grain sizes much smaller than 1 μm were systematically shown from the original experimental data. The UFG steels performed very high strength that reached to 2 ~ 4 times of the starting materials having conventionally coarse-grained structures. On the other hand, the uniform tensile elongation was commonly limited within a few percents when the materials have single-phased UFG structures. The limited uniform elongation was explained in terms of early plastic instability. On the basis of the understanding, the ways to manage both strength and ductility in the UFG steels were indicated.

Keywords: severe plastic deformation; thermomechanical processing; grain refinement strengthening; plastic instability; strain hardening

0 Introduction

Grain refinement has been always one of the most important subjects in microstructure control of structural metallic materials. However, the minimum mean grain size that has been conventionally achieved in bulky materials is around 10 μm. In case of commercial steels, the champion value has been 5 μm in the steel plate thermomechanically processed by so-called controlled rolling [1]. On the other hand, it has become recently possible to fabricate the steels with ultrafine grained (UFG) structures of which mean grain size is smaller than 1 μm, at least in laboratory scales [2]. One of the ways to obtain the UFG steel is thermomechanical processing under critical conditions, where phase transformation from heavily deformed austenite to ferrite is basically used. For example, grain sizes around 1 μm have been achieved in carbon steels through heavy one-pass deformation at low temperatures around 500 C in undercooled austenite region followed by rapid cooling [3]. The other route to realize the UFG structures is severe plastic deformation above logarithmic equivalent strain of about 4 [4]. The SPD can be applied not only to steels but also to most of workable metals and alloys, and the UFGs in 100 nm dimensions or even nanocrystals have been obtained in various kinds of metals and alloys [4].

The UFG materials perform the strength 2 ~ 4 times higher than that of the conventionally grain-sized materials [4,5]. On the other hand, however, the UFG materials usually exhibit limited ductility (especially limited uniform elongation) [4,5]. This imbalance between strength and ductility is the biggest issue of the UFG materials for practical application in the future. If the issue can be overcome, the UFG materials are quite attractive, because high strength can be achieved in simple chemical compositions without special alloying elements. The mechanical properties of the UFG materials have not yet been systematically clarified. In the present paper, strength and ductility of the UFG ferritic steels are systematically shown from the experimental evidences, and the way to manage both strength and ductility in the UFG steels is discussed.

1 Experimental

A Ti-added ultralow-carbon interstitial free (IF) steel was highly deformed by the accumulative roll-bonding (ARB) process, in order to obtain an UFG structure. The ARB is a kind of SPD process using rolling deformation, which was originally developed in the present author's group [4,6]. Fig. 1 illustrates the principle of the ARB process. Two pieces of the plain IF steel sheet 1 mm thick, 30 mm wide

and 300 mm long were stacked after degreasing and wire-brushing the contact surfaces. The stacked sheets were spot-welded at the top and tail ends, held in an electric furnace set at 500℃ for 600 s, and then roll-bonded by 50% one-pass rolling using a two-high rolling mill with a roll diameter of 310 mm without lubrication. The roll-bonded sheet was cut into two and the above mentioned procedures were repeated up to 7 cycles. Because von Mises equivalent strain for 50% rolling is 0.8, the total strain applied to the material by 7 cycles of the ARB is 5.6. The ARB processed sheets were annealed at various temperatures ranging from 400℃ to 800℃ for 1.8 ks to change the grain size.

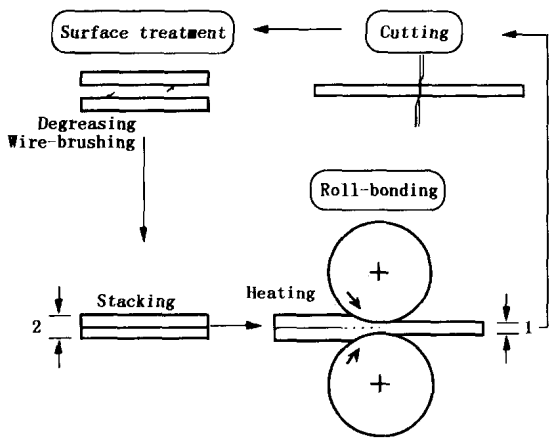

Fig. 1 Schematic illustration showing the principle of the ARB process

Another thermomechanical processing [7,8] was applied on a plain low-carbon steel (JIS-SS400) to fabricate another kind of UFG structure. The detailed procedures of the process were shown in the previous article [7]. The sheet of the SS400 having fully martensitic structure was obtained by austenitization and water-quenching. The martensite sheet was conventionally cold-rolled by 50% total reduction and annealed at various temperatures from 200℃ to 700℃ for 1.8 ks. By annealing under appropriate conditions, the UFG structures composed of UFG ferrite with mean grain size of 100 nm and nano-carbide dispersing within the UFG ferrite matrix uniformly can be formed [7,8]. This is a simple but novel process to obtain multi-phased UFG structure in carbon steels [7].

Microstructures of the obtained UFG steels were observed on the sections perpendicular to the transverse direction (TD) of the sheets by means of scanning electron microscopy (SEM), electron backscattering pattern analysis in a field-emission type SEM (FE-SEM/EBSP) and transmission electron microscopy (TEM). Mechanical properties of the specimens were measured in tensile test at room temperature and initial strain rate of 8.4×10^{-4} s^{-1}. Tensile specimen with gage width of 5 mm and gage length of 10 mm (1/5 miniature of JIS-5 specimen) was used for the tensile test. An extensometer was attached to the specimen in the tensile test, in order to measure exact displacement.

2 Mechanical properties of UFG steel with ferrite single phase

Fig. 2 shows the stress-strain curves of the IF steel ARB processed by various cycles. The strength of the sheet greatly increases by just 1 cycle of the ARB, while the tensile elongation significantly decreases. The strength rises up with increasing the ARB cycle and the tensile strength reaches to 900 MPa after 7 ARB cycles which is 3.2 times higher than that of the starting sheet (280 MPa). On the other hand, the elongation of the sheets shows nearly constant value after 1 ARB cycle. Especially, the uniform elongation is limited within a few %. These are typical mechanical properties of the SPD materials having single phase [6,9,10].

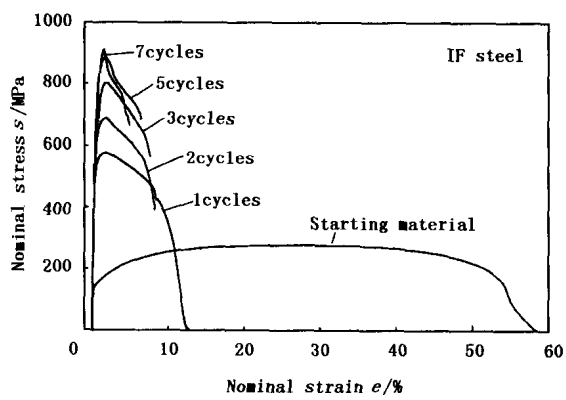

Fig. 2 Stree-strain curves of the IF steel ARB processed by various cycles at 500℃

A TEM microstructure of the IF steel ARB processed by 6 cycles is shown in Fig. 3. The ARB processed materials typically reveal the UFG microstruc-

ture elongated along the rolling direction (RD) of the sheets. The mean grain thickness in Fig. 3 was 210 nm. It has been already confirmed that the elongated UFGs are mostly surrounded by high-angle grain boundaries and the ARB processed sheets are uniformly filled with the elongated UFGs throughout thickness [11-14]. The material having such a microstructure performs very high strength but limited uniform elongation (Fig. 2).

When the ARB processed IF steel is annealed at various temperatures, a continuous change of the microstructures happens, which is called continuous recrystallization [5,15,16]. Fig. 4 shows TEM microstructures of the IF steel ARB processed by 5 cycles and then annealed at various temperatures for 1.8 ks. Through these processes, the bulky sheets of IF steel having various mean grain sizes ranging from 0.2 μm to 20 μm can be obtained, which are useful to test the mechanical properties of the UFG materials systematically.

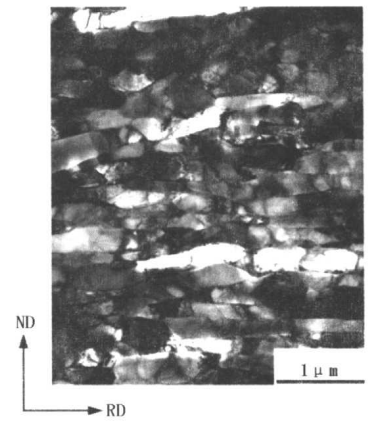

Fig. 3 TEM microstructure of the IF steel ARB processed by 6 cycles at 500℃. Observed from TD

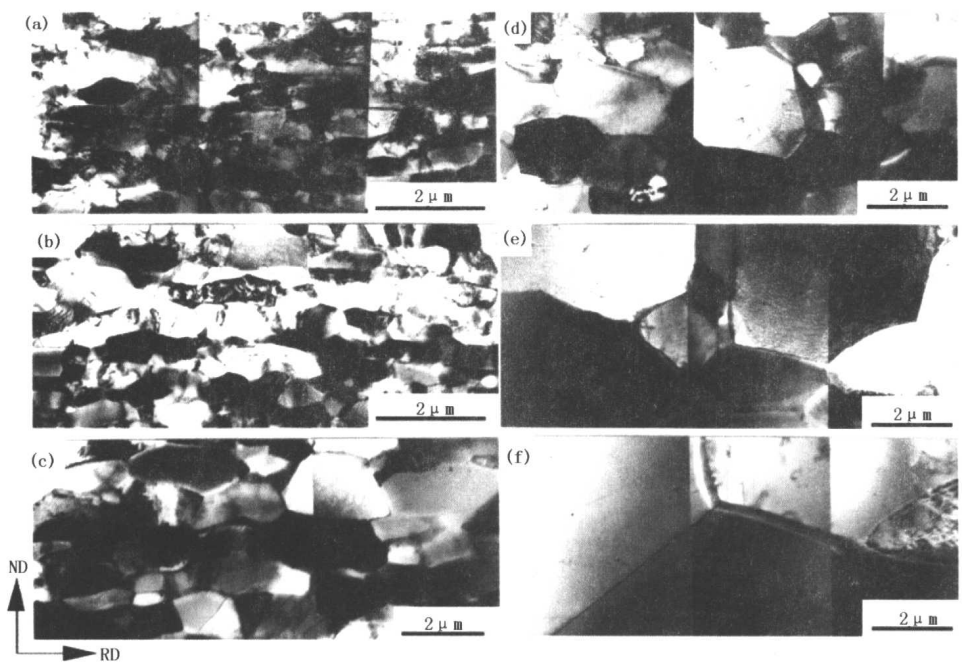

Fig. 4 TEDM microstructures of the IF steel ARB processed by 5 cycles at 500℃ and then annealed for 1.8 ks at (a)400℃; (b)500℃; (c)600℃; (d)625℃; (e)650℃ and (f)700℃. Observed from TD

Stress-strain curves of the IF steel with various mean grain sizes, which were fabricated by the ARB and annealing process, are shown in Fig. 5. The stress-strain behaviors changes as the mean grain size decreases. It is obvious that the flow stress, especially the yield stress, significantly increases with decreasing the grain size. On the other hand, the elongation, especially the uniform elongation, suddenly drops when the grain size becomes smaller than 1 μm. Uniform elongation in tensile test is determined as the strain at which macroscopicnecking initiates. Macroscopic necking is usually explained by plastic instability. Equation (1) indicates the well-known Considére criterion for plastic instability.

$$\sigma \geqslant \left(\frac{d\sigma}{d\varepsilon}\right) \tag{1}$$

此为试读,需要完整PDF请访问: www.ertongbook.com

According to this equation, necking initiates when the flow stress (left-hand term) becomes equal to the strain-hardening rate (right-hand term). The plastic instability is verified in the ultrafine grained IF steel with various mean grain sizes in Fig. 6. In Fig. 6, the dotted lines are the true stress-strain curves while the solid lines strain-hardening rate obtained by differentiating each stress-strain curve. The point at which two curves meet, i. e., the plastic instability point, coincided well with the uniform elongation of these specimens actually measured. That is, the limited uniform elongation in the UFG ferritic steel is understood in terms of plastic instability. As is shown in the stress-strain curves (Fig. 5), grain refinement significantly increases the yield strength of the material. On the other hand, strain-hardening is not enhanced by grain refinement, but it rather decreases with decreasing the grain size. As a result, plastic instability happens at very early stage of tensile test in the UFG ferritic material, resulting in limited uniform elongation. This is an inevitable nature of the UFG materials having single phase.

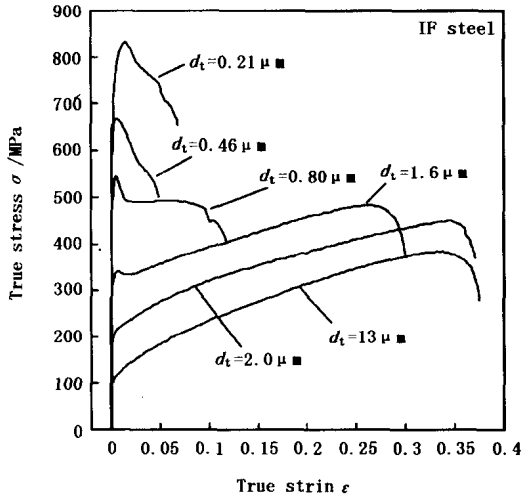

Fig. 5 True stress-strain curves of the IF steel with various mean grain sizes fabricated by the ARB and annealing process

3 Mechanical properties of multi-phased UFG steel

Understanding on the basis of plastic instability also tells us how to improve the ductility of the UFG materials. If the strain-hardening (right-hand term in eq. (1)) is enhanced by some means, it is expected

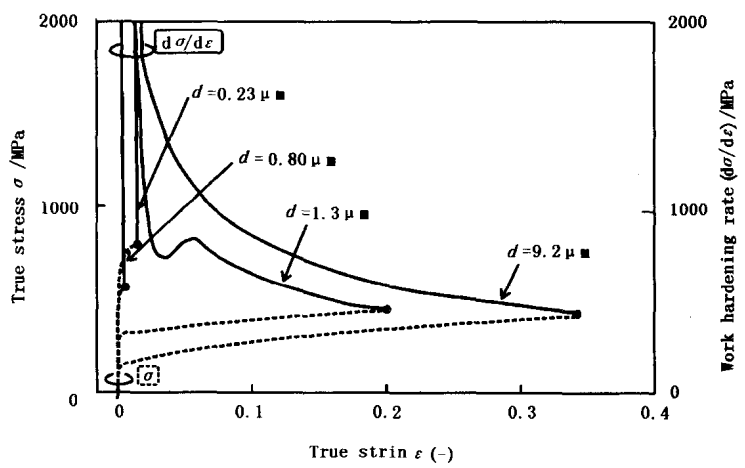

Fig. 6 True stress and strain-hardening rate as a function of true strain in the IF steel having various grain sizes fabricated by the ARB and annealing process

that the plastic instability is delayed even in the UFG material. One of the ways to enhance strain-hardening is to disperse fine second phase(s) within the UFG ferrite matrix uniformly. Fig. 7 is a TEM microstructure of the low-C steel (SS400) processed in the latter thermomechanical treatment (Martensite-method) [7]. The starting sheet having as-quenched martensite structure was conventionally cold-rolled by 50% and then annealed at 500℃ for 1.8 ks. The specimen shows a kind of UFG structure. It is noteworthy that a number of carbides with nano-meter sizes uniformly precipitate within the UFG ferrite matrix. This is because the as-quenched martensite was a supersaturated solid solution of carbon. Consequently, the structure resulted from the Martensite-method is a multi-phased UFG structure composed of

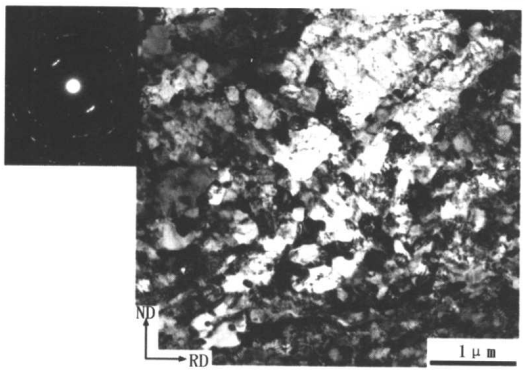

Fig. 7 TEM microstructure of the SS400 steel 50% cold-rolled and annealed at 773 K for 1.8 ks. Observed from TD. The starting microstructure was martensite

nearly equiaxed UFG ferrite having mean grain size of 100 nm and nano-carbides uniformly disperse within the UFG ferrite.

The multi-phased UFG steel fabricated by the Martensite-method actually managed both high strength and adequate ductility. Stress-strain curves of the low-C steel Martensite-processed are shown in Fig. 8. Strain-hardening is clearly enhanced and the specimen annealed at 550℃ showed tensile strength of 850 MPa, uniform elongation of 10% and total elongation of 10% at the same time. The standard tensile strength of this material is 400 MPa. The

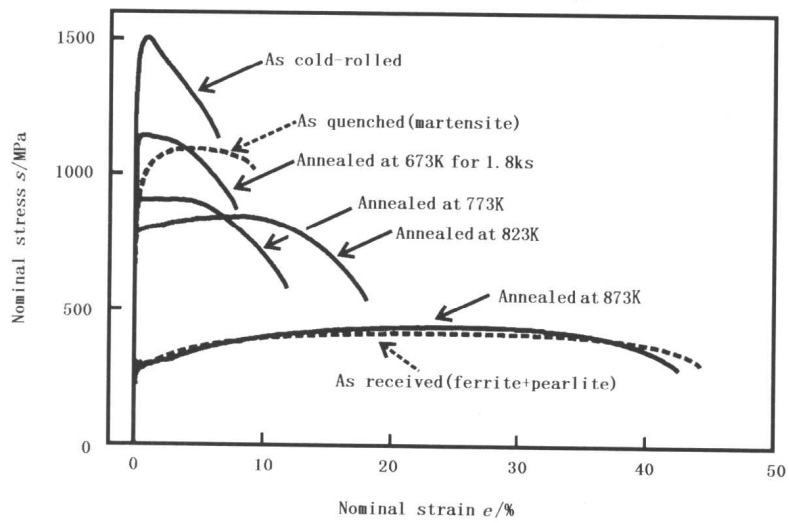

Fig. 8 Nominal stress-strain curves of the SS400 steel 50% cold-rolled and annealed at various temperatures for 1.8 ks. Starting microstructure was martensite

result clearly shows that dispersing fine precipitates is effective to manage both strength and ductility in the UFG steels.

4 Summary

Mechanical properties of UFG steels were shown based on the author's original experimental data. UFG steels perform very high strength but limited uniform tensile ductility when they have single phase structure. The limited uniform elongation was understood in terms of early plastic instability, which is an inevitable feature of the UFG single-phased materials. It was also indicated at the same time that dispersing nano-carbides within the UFG ferrite matrix is an effective way to improve the uniform elongation of the UFG steels. Steels have various options of multi-phased structure, such as, ferrite + cementite, ferrite + martensite, ferrite + bainite, and so on. The studies of the UFG steels should be focused on "multi-phase" in future.

References

[1] Maki T. Microstructure control by thermomechanical processing of steels. Netsusyori, 1989, 29 (5): 278 ~ 284

[2] Tsuji N. Ultrafine Grained Steels. Tetsu-to Hagané, 2002, 88 (7): 359 ~ 369

[3] Adachi Y, Tomita T, Hinotani S. Ferrite grain size refinement by heavy deformation during accelerated cooling in low-carbon steel. Tetsu-to Hagan , 1999, 85 (8): 620

[4] Tsuji N, Saito Y, Lee S-H *et al*. ARB (accumulative roll-bonding) and other new techniques to produce bulk ultrafine grained materials. Adv. Eng. Mater., 2003, 5 (5): 338 ~ 344

[5] Tsuji N, Ito Y, Saito Y *et al*. Strength and ductility of ultrafine grained aluminum and iron produced by ARB and annealing. Scripta Mater., 2002, 47: 893 ~ 899

[6] Saito Y, Tsuji N, Utsunomiya H *et al*. Ultra-fine grained bulk aluminum produced by accumulative roll-bonding (ARB) process. Scripta Mater., 1998, 39 (9): 1221 ~ 1227

[7] Tsuji N, Ueji R, Minamino Y *et al*. A new and simple process to obtain nano-structured bulk low-carbon steel with superior mechanical property. Scripta Mater., 2002, 46: 305 ~ 310

[8] Ueji R, Tsuji N, Minamino Y *et al*. Ultragrain refinement of plain low carbon steel by cold-rolling and annealing of martensite. Acta Mater., 2002, 50: 4177 ~ 4189

[9] Tsuji N, Saito Y, Utsunomiya H *et al*. Ultra-fine grained bulk steel produced by accumulative roll-bonding (ARB) process, Scripta Mater., 1999, 40 (7): 795 ~ 800

[10] Tsuji N, Ueji R, Ito Y *et al*. Possibility to manage both high strength and ductility in ultrafine grained structural metallic materials. Ultrafine Grained Materials IV, Eds. Zhu Y T, Langdon T G, Horita Z, Zehtbauer M J, Semiatin S L and Lowe T C. TMS, 2006: 81 ~ 88

[11] Tsuji N, Ueji R, Saito Y. Ultra-fine grains in ultra low carbon IF steel highly strained by ARB. Materia Japan, 2000, 39 (12): 961

[12] Tsuji N, Ueji R, Minamino Y. Nanoscale crystallographic analysis of ultrafine grained IF steel fabricated by ARB process. Scripta Mater., 2002, 47: 69 ~ 76

[13] Kamikawa N, Tsuji N, Minamino Y. Microstructure and texture through thickness of ultralow carbon IF steel sheet severely deformed by accumulative roll-bonding. Sci. Tech. Adv. Mater., 2004, 5: 163 ~ 172

[14] Li B L, Tsuji N, Kamikawa N. Microstructure homogeneity in various metallic materials heavily deformed by accumulative roll-bonding. Mater. Sci. Eng. A, 2006, in press

[15] Tsuji N, Ueji R, Ito Y *et al*. In-situ recrystallization of ultrafine grains in highly strained metallic materials. In: Proc. of the 21 st Risφ Int. Symp. On Mater. Sci.: Recrystallization - Fundamental Aspects and Relations to Deformation Microstructure, Hansen N, Huang X, Juul Jensen D, Lauridsen E M, Leffers T, Pantleon W, Sabin T J and Wert J A, eds. Risφ National Laboratory, Roskilde, Denmark, 2000: 607 ~ 616

[16] Tsuji N, Kamikawa N, Minamino Y. Effect of strain on deformation microstructure and subsequent annealing behavior of IF steel heavily deformed by ARB process. Mater. Sci. Forum, 2004, 467-470: 341 ~ 346

Grain Size Distribution Features and Yield Strength of Ultrafine-Grained Low Carbon Steels

Fuxing YIN [1], *Noriyuki TSUCHIDA* [2] *Kotobu NAGAI* [1]
(1. **Steel Research Center, National Institute of Materials Science, Tsukuba**, 305 - 0047, **Japan**; 2. **Department of Materials Science and Chemistry, University of Hyogo, Himeji**, 671 - 2280, **Japan**)

Abstract: Caliber - rolling of low - carbon steels in ferrite temperature range shows a high efficiency in producing an ultrafine ferrite/cementite microstructure in low - carbon steels. In order to clarify the microstructural contributions to the yield strength of the ultrafine - grained steel, grain size distribution and average grain size were obtained for the as - rolled sample and the annealed samples, all of which show a nominal grain size <1 μm. With grain size distribution analysis the average grain size for 5° grain boundary definition is found to be similar to nominal grain size observed with SEM, while that for 15° definition is about 2 time of nominal grain size. Reduced yield strengths for the three as - rolled and annealed samples are calculated by deleting the contributions of dislocation strengthening and cementite dispersion strengthening, respectively. It is found that the k parameter in Hall - Petch plots becomes much lower when the low - angle boundaries are included. When the strengthening effect of only a fraction of dislocations is considered a k parameter similar to the reported one can be obtained with the average grain size at 15° grain boundary definition.

Keywords: ultrafine - grained steel; grain size distribution; orientation imaging microscopy (OIM); yield strength; dislocation

0 Introduction

A lot of severe plastic deformation (SPD) processes have been investigated that produce an average ferrite grain size of ~1 μm in low - carbon steels [1,2]. As a kind of SPD process, caliber - rolling of low - carbon steels in ferrite temperature range shows a high efficiency in producing an ultrafine ferrite/cementite microstructure in low - carbon steels [3]. It was found that warm - rolling induced not only the ultrafine ferrite microstructure in the steel, but also the high dislocation density, the preferred grain orientation, as well as the fine dispersion of cementite particles. As compared with the 20 μm ferrite/pearlite microstructure for the same SM490 steel, the increase of yield strength in the caliber - rolled 3 μm ferrite/cementite microstructure was contributed by grain refinement, dislocation and cementite dispersion in the value of 312.5, 115 and 55.2 MPa, respectively. It is indicated that both grain refinement and dislocation introduction make a contribution to the increase of yield strength in the plastically deformed microstructure.

On the other hand, an average grain size is usually applied to characterize the changes of yield-strength with Hall - Petch relationship, and the correct estimation of the average grain size becomes quite important for ultrafine grained microstructure since a larger deviation in yield strength is caused by that of grain size when the grain size becomes smaller. Recently, a multi - pass warm - rolling and the following annealing were used to fabricate the ultrafine ferrite/cementite microstructure with an average grain size of <1 μm[4]. It was proposed that for the ultrafine microstructure the Hall - Petch relationship was still remained with $\sigma_0 = 175$ MPa and $k = 475$ MPa · $\mu m^{1/2}$. The nominal average grain size of the ferrite microstructure was measured with SEM observation and was applied to the linear Hall - Petch relationship fitting. However, the formation of ultrafine ferrite microstructure is the product of dynamic recrystallization process during the warm -

rolling. In the recrystallized Al the distribution of grain volume was described by a lognormal distribution, and the standard deviation of $\ln(d)$ varied in the range of 0.33 ~ 0.76 [5]. There has been rare report on the effects of grain size distribution on the yield strength of steel, and it is considered that the broad grain size distribution in the ultrafine grain microstructure may influence the tensile behavior considerably. In the present work, the grain size distribution is derived with Orientation Imaging Microscopy (OIM) analysis for the multi - pass caliber - rolled steel with the nominal average grain size of < 1 μm. The dependence of yield strength on the average grain size is discussed based on the different grain boundary definitions and the effects of dislocations.

1 Experimental procedure

A low - carbon steel with the composition equivalent to JIS - SM490 (0.15C - 0.3Si - 1.43Mn mass%) was used in the present work. The hot - rolled steel bar with a 80 mm × 80 mm square section was hold at 1 173 K for 3.6×10^3 s and quickly cooled to 773 K. The fist pass caliber rolling was conducted at 773 K at a section area reduction of 91%, and steel bars with a 24 mm × 24 mm square section were obtained. Then the bars were cooled to 723 K and the second pass caliber rolling was conducted at a section area reduction of 43.8%. The final section area of the rolled steel bars is 18 mm × 18 mm, and those steel bars are hereafter named as AS sample. The as - rolled steel bars were then annealed for 3.6×10^3 s at 743 K and 773 K, respectively. The nominal grain size for the annealed samples was 0.5 and 0.7 μm, and the samples are hereafter called as 05 C and 07 C.

Tensile test was conducted at 296 K at a strain rate of $3.3 \times 10^{-4}\ s^{-1}$ in bar specimens with a diameter of 3.5 mm and gauge length of 25 mm. Microstructure of the samples on the RD section was analyzed with LEO - 1550 SEM equipped with EBSD system (TSL Inc.). Grain size distribution was obtained by defining grain boundary at the misorientation of 5° and 15°, respectively. Meanwhile, the kernel average misorientation distribution image was also obtained by the nearest neighboring pixel calculation at a step of 50 nm.

2 Experimental results and discussion

Fig. 1 shows the stress - strain curves of the three samples during tensile test at 296 K. All the samples show the obvious difference between upper and lower yield stresses, while the lower yield stress was sustained to 5% strain in all the samples with little strain strengthening. The lower yield strength is 933, 870 and 770 MPa, respectively for AS, 05 C and 07 Csamples. Fig. 2 shows the OIM microstructure of the samples obtained with EBSD measurement. Homogeneous polygonal grain structure occurs in the samples when the grain boundaries with a misorientation > 5° are considered, while some of the grains with a misorientation > 15° show the irregular shapes. Fig. 3 shows the grain size distribution by area - weighted fraction in two different grain boundary definitions. In the case of 5° grain boundaries grain size distribution can well be fitted with the lognormal function. In contrast there are some grains with the larger areas that deviate from lognormal distribution in the case of 15° grain boundary definition.

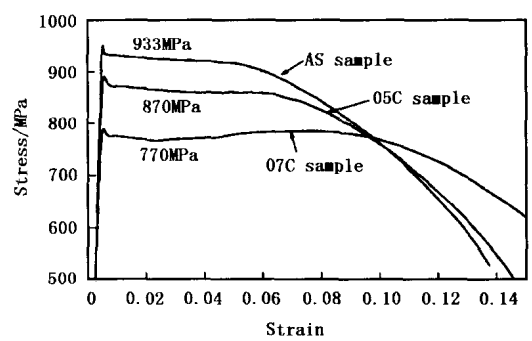

Fig. 1 The stress - strain curves of the AS, 05 C and 07 C samples obtained by tensile tests

There are two parameters that are necessary to characterize the lognormal distribution of grain size, x_c and w. x_c indicate the center value of $\ln(d)$ distribution and w is the standard deviation of $\ln(d)$. When the grain size abides by the lognormal distribution the average grain size, d_0 can be calculated by $x_c \cdot \exp(1/2w^2)$ through a correction of area -

weighted fraction to the normal number – weighted fraction [6]. Table 1 shows the results of the fitted grain size distribution in the two cases of grain boundary definition. The average grain sizes, d_0 derived from the grain size distributions are different according to the grain boundary definitions, and the grain size at 15° definition is about 1.5 ~ 1.8 times larger than that calculated at 5° definition. Meanwhile the variance of grain size distribution is also obtained with the fitted standard deviation parameter, and the variance is about 0.15 ~ 0.2 μm at 5° definition and that becomes quite larger at 15° definition. On the other hand, grain size distribution at 15° definition indicates a bimodal character and the fitting has ignored the grains with larger grain sizes, whose area – weighted fraction deviate from the lognormal distribution. Therefore the average grain size at 15° definition should be a little larger than the values shown in table 1.

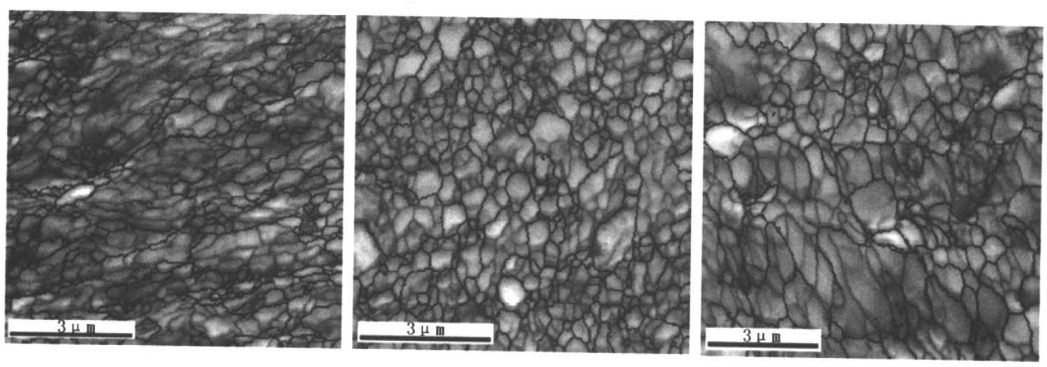

Fig. 2 OIM microstructure of the AS, 05 C and 07 C samples with the contrast of image quality obtained in EBSD measurement. The grain boundaries with a misorientation >15° in indicated by the dark lines and the grey lines indicate the boundaries of 5° ~ 15°

Table 1 The average grain size and its variance obtained from lognormal fitting of the erea-weighted grain size fraction

Sample		x_c	w	d_0/μm	Variance/μm	Nominal d/μm
5°Grain boundary	AS	1.512	0.906	0.54	0.189	0.40
	05C	1.349	0.782	0.57	0.154	0.47
	07C	2.105	0.761	0.78	0.200	0.70
15°Grain boundary	AS	2.702	0.664	0.80	0.159	0.40
	05C	2.225	0.904	1.05	0.364	0.47
	07C	3.143	0.917	1.33	0.473	0.70

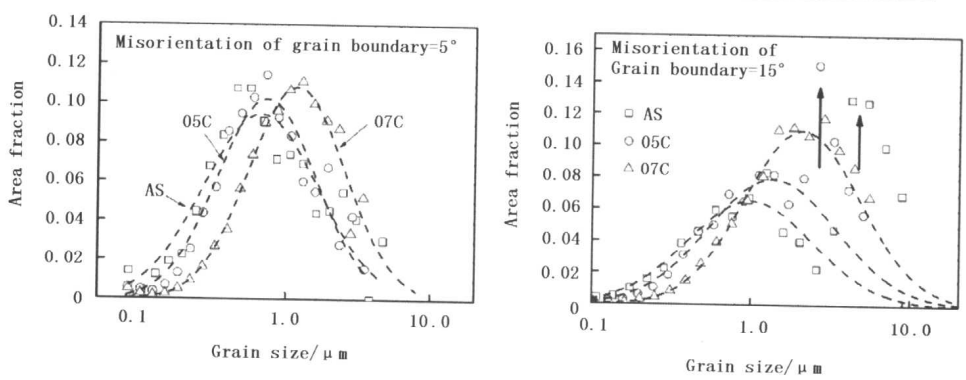

Fig. 3 The area – weighted fractions of three samples in two different grain boundary definitions. The dashed lines show the lognormal fitting results of the distributions

When considering the Hall – Petch relationship in those samples the contributions of dislocation and cementite dispersion to yield strength should be divided from the measured data. By applying the mod-

此为试读,需要完整PDF请访问: www.ertongbook.com